GEOPHYSICS, VOL. 72, NO. 1 (JANUARY-FEBRUARY 2007); P. S25–S31, 8 FIGS.
10.1190/1.2399368

A separable-kernel decomposition method for approximating the DSR continuation operator

Jing-Bo Chen[1], Hong Liu[1], and Zhi-Fu Zhang[1]

ABSTRACT

We develop a separable-kernel decomposition method for approximating the double-square-root (DSR) continuation operator in one-way migrations in this paper. This new approach is a further development of separable approximations of the single-square-root (SSR) operator. The separable approximation of the DSR operator generally involves solving a complicated nonlinear system of integral equations. Instead of solving this nonlinear system directly, our new method consists of repeatedly applying the separable-kernel technique developed for the two-variable SSR operator to the multivariable DSR operator. Numerical experiments demonstrate the efficiency of the proposed method. We illustrate the fast convergence of the obtained separable approximation. We also demonstrate the capability of this novel approximation for imaging an area with geologic complexities through synthetic data.

INTRODUCTION

Wave-equation, prestack depth migration plays a very important role in imaging regions with geologic complexities. Most of the wave-equation migration algorithms are based on the Taylor or Padé approximations for the one-way wave operator, such as the finite-difference method (Claerbout, 1985), the split-step Fourier method (Stoffa et al., 1990), the Fourier finite-difference method (Ristow and Rühl, 1994), and the generalized-screen method (Le Rousseau and de Hoop, 2001). The generalized-screen method uses two Taylor approximations and a perturbation hypothesis to approximate the one-way wave operator by products of functions in space variables and functions in wavenumber variables. This approximation enables the Fourier transform in wavenumber domain to be independent of the space variables, thus resulting in great improvement on the computational efficiency. In spite of its great success, this method suffers a slow convergence, resulting from the perturbation hypothesis and Taylor approximations.

Recently, Chen and Liu (2004) developed a method for constructing optimal separable approximations for the SSR continuation operator. This new method is based on an optimization procedure and a separable-kernel decomposition technique. It preserves the advantages of the generalized-screen method, while having fast convergence. Numerical comparisons demonstrate the advantages of optimal separable approximation over the generalized-screen method in Chen and Liu (2006).

Many important wave-equation, prestack, depth-migration algorithms are based on the DSR continuation operator, such as the prestack migration by split-step DSR (Popovici, 1996), the 3D prestack migration of common-azimuth data (Biondi and Palacharla, 1996), and offset-domain pseudoscreen prestack depth migration (Jin et al., 2002). Therefore, it will be useful to develop optimal separable approximations for the DSR continuation operator by generalizing the methodology introduced by Chen and Liu (2004, 2006). The optimal separable approximation for the SSR continuation operator involves two variables and can be achieved by numerically solving a linear system of integral equations. For the DSR continuation operator, however, four or six variables are involved. As a result, the integral kernel contains the multiplication of three or five functions and a nonlinear integral system arises. Therefore, we must solve a nonlinear system of integral equations by numerical methods. This is a difficult task, since numerical techniques could require long computation time to converge to the true solution of a nonlinear problem (Ortega and Rheinboldt, 1970). To overcome these difficulties, we will present a simple, but efficient separable-kernel decomposition method in this paper. The basic idea of this method is to repeatedly apply the separable-kernel technique developed for the two-variable SSR operator to the multivariable DSR operator. The obtained approximation has two important features that can result in a significant improvement on computational efficiency. One is that we can use the fast Fourier transform (FFT) algorithm, which is independent of space variables; the other is that we can implement

Manuscript received by the Editor April 18, 2006; revised manuscript received September 11, 2006; published online December 13, 2006.
[1]Chinese Academy of Sciences, Institute of Geology and Geophysics, P. O. Box 9825, Beijing 100029, China. E-mail: chenjb@mail.iggcas.ac.cn; liuhong@mail.iggcas.ac.cn; zfzhang@mail.iggcas.ac.cn.

high-dimensional FFT by independent low-dimensional FFT.

In the next section, we will give a brief review of the optimal separable approximation for the SSR operator. This is followed by the presentation of the separable-kernel decomposition method for the DSR continuation operator. We then perform numerical experiments to analyze the approximation accuracy and test the feasibility of the obtained new approximations.

OPTIMAL SEPARABLE APPROXIMATION FOR THE SSR OPERATOR

To facilitate our discussion about the DSR operator, we first briefly review the optimal separable approximation for the SSR operator given by Chen and Liu (2004, 2006). We then discuss some related issues.

Consider the SSR continuation operator in frequency-wavenumber domain

$$\mathcal{A}(x,y;k_x,k_y) = \exp\left\{ i\sqrt{\frac{\omega^2}{c(x,y,z)^2} - (k_x^2 + k_y^2)}\Delta z \right\}, \tag{1}$$

where ω is the frequency, k_x and k_y are wavenumbers, $c(x,y,z)$ is the wave velocity, and Δz is the continuation depth. For the sake of brevity, we set $u = \omega/c$ and $k = \sqrt{k_x^2 + k_y^2}$. Then the one-way operator 1 becomes

$$\mathcal{A}(u,k) = \exp\{i\sqrt{u^2 - k^2}\Delta z\}. \tag{2}$$

The optimal separable approximation for operator 2 is to find functions $\phi(u)$, $\psi(k)$, and a complex number λ such that

$$\min_{\tilde{\phi},\tilde{\psi},\tilde{\lambda}} \|\mathcal{A}(u,k) - \tilde{\lambda}\tilde{\phi}(u)\tilde{\psi}(k)^*\|_{L^2} = \|\mathcal{A}(u,k) - \lambda\phi(u)\psi(k)^*\|_{L^2}, \tag{3}$$

where * denotes the complex conjugate, $\tilde{\lambda}$ is an arbitrary complex number, and

$$\tilde{\phi} \in \{\tilde{\phi}(u):\tilde{\phi}(u) \in L^2[a,b], \|\tilde{\phi}(u)\|_{L^2} = 1\}, \tag{4}$$

$$\tilde{\psi} \in \{\tilde{\psi}(k):\tilde{\psi}(k) \in L^2[c,d], \|\tilde{\psi}(k)\|_{L^2} = 1\}. \tag{5}$$

Here, a and b are the lower and upper limits of u determined by the frequency and velocity involved in a geologic area; c and d are the lower and upper limits of the wavenumber in the same problem under consideration. We denote by $L^2[a,b]$ the space consisting of square integral functions defined on $[a,b]$. The norm $\|\cdot\|_{L^2}$ is defined as

$$\|f(x)\|_{L^2} = \left(\int_a^b |f(x)|^2 dx \right)^{1/2}, \quad \forall\, f(x) \in L^2[a,b]. \tag{6}$$

In equations 4 and 5, we require that both the function in space and the function in wavenumber be normalized to be unit in the sense of the norm $\|\cdot\|_{L^2}$. Using the Lagrange multiplier, we can easily prove that the solution to problem 3 is the eigenfunction of the following linear system of integral equations (see Appendix A for a proof):

$$\int_c^d \mathcal{A}(u,k)\psi(k)dk = \lambda\phi(u),$$

$$\int_a^b \mathcal{A}(u,k)^*\phi(u)du = \lambda^*\psi(k). \tag{7}$$

Consider partitions of intervals $[a,b]$ and $[c,d]$ with nodes

$$u_i = a + (i-1)\Delta u, \quad i = 1,2,\ldots,m+1; \quad \Delta u = \frac{b-a}{m}, \tag{8}$$

$$k_j = c + (j-1)\Delta k, \quad j = 1,2,\ldots,n+1; \quad \Delta k = \frac{d-c}{n}. \tag{9}$$

Set $\phi = (\phi_1,\phi_2,\ldots,\phi_m)^T$ and $\psi = (\psi_1,\psi_2,\ldots,\psi_n)^T$, where $\phi_i = \phi(u_i), i = 1,2,\ldots,m$ and $\psi_j = \psi(k_j), j = 1,2,\ldots,n$. Further, let $A = (a_{i,j})$ be a matrix with entries

$$a_{i,j} = \mathcal{A}(u_i,k_j), \quad i = 1,2,\ldots,m; \quad j = 1,2,\ldots,n. \tag{10}$$

Using the theory of singular-value decomposition (Chen and Liu, 2004), we can show that ϕ and ψ are the left and right singular vector of A corresponding to the maximum singular value λ_1, respectively. Let $\phi^{(1)}(u)$ and $\psi^{(1)}(k)$ denote the interpolation function of ϕ and ψ, respectively. The interpolation function is an approximation to the original function and has the same values as the original function at the discrete points. Usually, piecewise linear interpolation works well. Namely, we have

$$\phi^{(1)}(u) = \frac{u-u_i}{u_{i-1}-u_i}\phi_{i-1} + \frac{u-u_{i-1}}{u_i-u_{i-1}}\phi_i, \quad u_{i-1} \le u \le u_i, \quad i = 2,3,\ldots,m, \tag{11}$$

$$\psi^{(1)}(k) = \frac{k-k_j}{k_{j-1}-k_j}\psi_{j-1} + \frac{k-k_{j-1}}{k_j-k_{j-1}}\psi_j, \quad k_{j-1} \le k \le k_j, \quad j = 2,3,\ldots,n. \tag{12}$$

In practical application, we only need the values of the original function at the discrete points. Therefore, this substitution loses no accuracy for practical application.

The optimal separable approximation for $\mathcal{A}(u,k)$ is thus obtained:

$$\mathcal{A}(u,k) \simeq \lambda_1\phi^{(1)}(u)\psi^{(1)}(k)^*. \tag{13}$$

Repeating this process, we can obtain optimal separable approximation for $\mathcal{A}(u,k)$:

$$\mathcal{A}(u,k) \simeq \sum_{l=1}^{L} \lambda_l\phi^{(l)}(u)\psi^{(l)}(k)^*, \tag{14}$$

where $L \le r$ and r is the rank of A. For details, see Chen and Liu (2006).

Using equation 14 as an approximation of the one-way, wave-extrapolation operator, we can construct a corresponding migration al-

gorithm. The migration procedure is the same as that of the generalized-screen method (Le Rousseau and de Hoop, 2001).

From the above discussion, we can see that the optimal separable approximation for the SSR continuation operator consists of two steps. The first step is an optimization problem. The second step is, in fact, a separable-kernel decomposition technique (Pipkin, 1991; Song, 2001).

In practice, a normalizing procedure applies to equation 14 in the same way as used in Le Rousseau and de Hoop (2001) to guarantee stability. Usually, for $L \geq 4$, equation 14 achieves very high accuracy, and the error induced by the normalization is negligible (Chen and Liu, 2004, 2006).

Notice that each component in equation 14 is a global approximation over the entire wavenumber domain. This means that each component accounts for energy propagating in all downward directions. This property is an advantage of the global-approximation approach.

Usually, it is expensive to solve the problem of singular-value decomposition. Fortunately, however, equation 14 can be made independent of the migration process. Therefore, we can compute equation 14 in advance and restore it for subsequent use in migration. Fast singular-value decomposition algorithms are available and their complexity analysis is well established (Stoer and Bulirsch, 1993). Another advantage in our situation is that we do not need to compute all singular values and the corresponding singular vectors. Usually, it is enough to obtain the first few components in equation 14, which means a significant saving in computational cost.

SEPARABLE-KERNEL DECOMPOSITION FOR THE DSR OPERATOR

Consider the 2D DSR continuation operator in frequency-wavenumber domain and in midpoint-offset coordinates (Claerbout, 1985):

$$\mathcal{B}_2(u_r,u_s,k_m,k_h) = \exp\left\{ i\left(\sqrt{u_r^2 - \frac{1}{4}(k_m + k_h)^2} + \sqrt{u_s^2 - \frac{1}{4}(k_m - k_h)^2}\right)\Delta z\right\}, \quad (15)$$

where $u_r = \omega/v_r$, $u_s = \omega/v_s$, and v_r and v_s are the velocities at receiver and shot locations, respectively; m and h are the midpoint and offset coordinates, respectively; and k_m and k_h are the corresponding wavenumbers. The midpoint-offset coordinates are related to the shot-receiver coordinates through the following relations

$$m = \frac{r+s}{2}, \quad h = \frac{r-s}{2}. \quad (16)$$

As in the case of the SSR operator, the optimal separable approximation for operator 15 is to find functions $\phi(u_r)$, $\varphi(u_s)$, $\psi(k_m)$, $\xi(k_h)$, and a complex number λ such that

$$\min_{\tilde{\phi},\tilde{\varphi}\tilde{\psi},\tilde{\xi},\tilde{\lambda}} \|\mathcal{B}_2 - \tilde{\lambda}\tilde{\phi}(u_r)\tilde{\varphi}(u_s)^*\tilde{\psi}(k_m)^*\tilde{\xi}(k_h)\|_{L^2} = \|\mathcal{B}_2(u_r,u_s,k_m,k_h) - \lambda\phi(u_r)\varphi(u_s)^*\psi(k_m)^*\xi(k_h)\|_{L^2}, \quad (17)$$

where * denotes the complex conjugate, $\tilde{\lambda}$ is an arbitrary complex number, and

$$\|\tilde{\phi}(u_r)\|_{L^2} = \|\tilde{\varphi}(u_s)\|_{L^2} = \|\tilde{\psi}(k_m)\|_{L^2} = \|\tilde{\xi}(k_h)\|_{L^2} = 1. \quad (18)$$

Similarly, problem 17 is equivalent to the following eigenvalue problem of a nonlinear system of integral equations

$$\begin{aligned}
&\int \mathcal{B}_2\varphi(u_s)\psi(k_m)\xi(k_h)^* du_s dk_m dk_h = \lambda\phi(u_r),\\
&\int \mathcal{B}_2^*\phi(u_r)\psi(k_m)^*\xi(k_h) du_r dk_m dk_h = \lambda^*\varphi(u_s),\\
&\int \mathcal{B}_2^*\phi(u_r)\varphi(u_s)^*\xi(k_h) du_r du_s dk_h = \lambda^*\psi(k_m),\\
&\int \mathcal{B}_2\phi(u_r)^*\varphi(u_s)\psi(k_m) du_r du_s dk_m = \lambda\xi(k_h). \quad (19)
\end{aligned}$$

The above nonlinear system of integral equations is very difficult to be numerically solved directly. We now present an efficient and accurate approximate method. The basic idea is to repeatedly apply the separable-kernel technique for operators in two variables to the present DSR continuation operator, which involves four variables.

Set $\mathbf{u} = (u_r,u_s)$ and $\mathbf{k} = (k_m,k_h)$, and we regard $\mathbf{u}$ and $\mathbf{k}$ as a single variable, respectively. Thus, we are left with a two-variable operator $\mathcal{B}_2(\mathbf{u},\mathbf{k})$. Now we seek the optimal separable approximation for $\mathcal{B}_2(\mathbf{u},\mathbf{k})$ by $\alpha(\mathbf{u})$ and $\beta(\mathbf{k})$. According to the result for the SSR operator, we have

$$\mathcal{B}_2(\mathbf{u},\mathbf{k}) \simeq \sum_{l=1}^{L} \lambda_l \alpha^{(l)}(\mathbf{u})\beta^{(l)}(\mathbf{k})^*. \quad (20)$$

Approximation 20 itself is very useful, because it separates the space variables and wavenumber variables. This separation makes it possible to perform FFT with respect to wavenumber independently of the space variables in seismic migration, which forms the core of the generalized-screen method.

Now let us proceed further. For each $\beta^{(l)}(\mathbf{k}) = \beta^l(k_m,k_h)$, using the result for the SSR operator again, we obtain

$$\beta^l(k_m,k_h) \simeq \sum_{i=1}^{I} \lambda_l^i \psi_i^{(l)}(k_m)\xi_i^{(l)}(k_h)^*. \quad (21)$$

Combining equations 20 and 21, we obtain another approximation

$$\mathcal{B}(\mathbf{u},k_m,k_h) \simeq \sum_{l=1}^{L}\sum_{i=1}^{I} \lambda_l(\lambda_l^i)^*\alpha^{(l)}(\mathbf{u})\psi_i^{(l)}(k_m)^*\xi_i^{(l)}(k_h). \quad (22)$$

In addition to the separation of the space variables and wavenumber variables, the two wavenumber variables are further separated in approximation 22. The benefit of this further separation is that we can perform a 2D FFT by two independent 1D FFTs, which means a significant reduction of computational cost. Usually, the approximation achieves good accuracy for $L = 4$ and $I = 2$.

Further, for each $\alpha^{(l)}(\mathbf{u}) = \alpha^l(u_r,u_s)$, we obtain again

$$\alpha^l(u_r,u_s) \simeq \sum_{j=1}^{J} \tilde{\lambda}_l^j \phi_j^{(l)}(u_r)\varphi_j^{(l)}(u_s)^*. \quad (23)$$

Combining equations 23 and 22, we finally arrive at

$$\mathcal{B}_2(u_r,u_s,k_m,k_h) \simeq \sum_{j=1}^{J}\sum_{l=1}^{L}\sum_{i=1}^{I} \lambda_l(\lambda_l^i)^*\tilde{\lambda}_l^j\phi_j^{(l)}(u_r)\varphi_j^{(l)}(u_s)^*\psi_i^{(l)} \times(k_m)^*\xi_i^{(l)}(k_h). \quad (24)$$

Now, consider the 3D DSR continuation operator in frequency-wavenumber domain

$$\mathcal{B}_3(\mathbf{u},\mathbf{k}_1,\mathbf{k}_2) = \exp\left\{ i\left(\sqrt{u_r^2 - \frac{1}{4}(k_{mx}+k_{hx})^2 - \frac{1}{4}(k_{my}+k_{hy})^2} + \sqrt{u_s^2 - \frac{1}{4}(k_{mx}-k_{hx})^2 - \frac{1}{4}(k_{my}-k_{hy})^2}\right)\Delta z\right\}, \quad (25)$$

where (mx,my) and (hx,hy) are midpoint and offset coordinates, respectively, and $\mathbf{k}_1 = (k_{mx},k_{my})$ and $\mathbf{k}_2 = (k_{hx},k_{hy})$ are the corresponding wavenumber vectors.

Regarding $\mathbf{u}$, $\mathbf{k}_1$, and $\mathbf{k}_2$ as a single variable, respectively, and using equation 22, we obtain separable approximation for the 3D DSR continuation operator

$$\mathcal{B}_3(\mathbf{u},\mathbf{k}_1,\mathbf{k}_2) \simeq \sum_{l=1}^{L}\sum_{i=1}^{I} \lambda_l(\lambda_l^i)^*\alpha^{(l)}(\mathbf{u})\psi_i^{(l)}(\mathbf{k}_1)^*\xi_i^{(l)}(\mathbf{k}_2). \quad (26)$$

Based on the results obtained in Chen and Liu (2004), we know that approximation 26 can achieve a very high accuracy for very small L and I. For DSR-based, 3D wave-equation, prestack depth migrations, it is crucial to compute the FFT with respect to operator 25 efficiently. Directly using operator 25, we need to compute $M \times M$ 4D FFTs, where M is the number of different velocities in a certain geologic area. This requires a considerable computational effort. While using approximation 26, we only need to compute $2 \times L \times I$ independent 2D FFTs, and L and I depend only on the velocity range in a certain geologic area, which is independent of the number of different velocities in that area. Therefore, using approximation 26 can result in a significant improvement on computational efficiency, in particular, for a large number M. For example, for the velocity range 3000–5000 m/s, we can take $L = 4$ and $I = 2$. Therefore, no matter how large M is, we only need to compute 16 independent 2D FFTs when using approximation 26. On the other hand, when supposing $M = 5$ (or larger) and using operator 25, we need to compute 25 (or more) 4D FFTs.

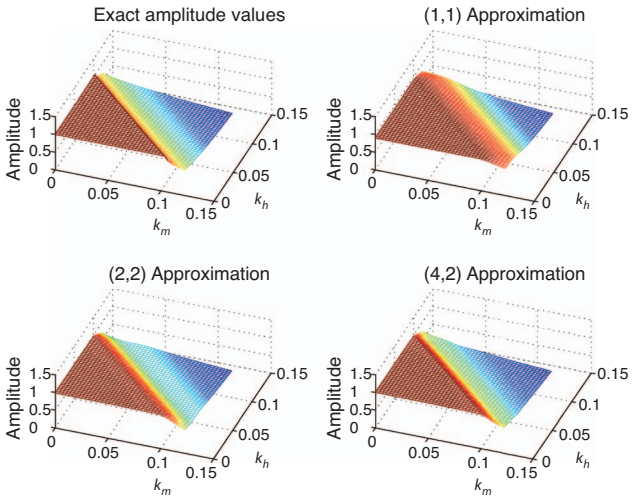

Figure 1. The exact-amplitude values of $\mathcal{B}_2(u(2,20),k_m,k_h)$, (1, 1), (2, 2), and (4, 2) approximations.

NUMERICAL EXPERIMENTS

For simplicity of illustrations, we approximate the 2D DSR continuation operator 15 using the separable approximation 22. We denote approximation 22 as the (L,I) approximation. Here, L denotes the number of approximation order in the first-step separable approximation, and I denotes the number of approximation order in the second-step separable approximation.

In practical applications, we only need to evaluate the values of operator 15 at discrete grid points. It can be shown that approximation 22 converges to operator 16 at these grid points by using the singular-value decomposition theory. However, when the grid becomes gradually finer, we can also show that approximation 22 converges to operator 16 at any point. For details, see Chen and Liu (2004) and references therein. In the following experiments we will focus on the rate of convergence.

We consider a depth interval with lateral-velocity variations. The minimum velocity and maximum velocity at this interval are 3000 and 5000 m/s, respectively. We choose $\omega = 80\pi$. Therefore, the varying range of u_r and u_s is $[80\pi/5000, 80\pi/3000]$. The varying range of wavenumber k_m and k_h is chosen both as $[0, \pi/25]$. Further, we take $\Delta u_r = \Delta u_s = (\pi/750 - \pi/1250)$ and $\Delta k_m = \Delta k_h = \pi/1000$. Define $u_r(i) = 40\pi/2500 + (i-1)\Delta u_r, i = 1,2,\ldots,21$, and for u_s, k_m, and k_h, we make the same definitions.

In Figure 1 we show the exact amplitude values of $\mathcal{B}(u(2,20),k_m,k_h)$, as well as the (1, 1), (2, 2), and (4, 2) approximations of the exact amplitude values. Here, $u(2,20) = (u_r(2),u_s(20))$. We see that the (1, 1) approximation describes the basic geometry of the exact-amplitude values. The exact-amplitude values consist of two parts. For nonevanescent waves, they are equal to 1; for evanescent waves, they are less than 1. The (1, 1) approximation characterizes both nonevanescent and evanescent waves. For the (4, 2) approximation, good accuracy has been achieved. Figure 2 shows the corresponding results for the phase. Notice that the (1, 1) approximation also accounts for both nonevanescent and evanescent waves in terms of the phase.

In order to show the amplitude variation more clearly, we show three 2D slices of Figure 1 for fixed k_h, fixed k_m, and for $k_m = k_h$ in Figures 3–5.

To describe the errors quantitatively, we have computed the relative errors:

$$\text{error} = \left[\frac{1}{T}\sum_{i=1}^{40}\sum_{j=1}^{40}|\mathcal{B}_2((2,20),k_m(i),k_h(j)) - \tilde{\mathcal{B}}_2|^2\right]^{1/2}, \quad (27)$$

where

$$T = \sum_{i=1}^{40}\sum_{j=1}^{40} |\mathcal{B}_2((2,20),k_m(i),k_h(j))|^2$$

and

$$\tilde{\mathcal{B}}_2 = \sum_{l=1}^{s}\sum_{n=1}^{t} \lambda_l(\lambda_l^n)^* \alpha^{(l)}(\mathbf{u}(2,20))\psi_n^{(l)}(k_m)^*\xi_n^{(l)}(k_h).$$

In our experiment, we find that the errors are mainly caused by the first step (L step) approximation. For the second step (I step), for $I = 2$, we have already obtained very good accuracy for a large L, say $L = 4$ (Figure 6). For larger I, we can obtain a similar result. This is because the second-step approximation is performed on the basis of the first-step approximation, and the contributions from larger I account for only a small fraction of the total approximation. This simple experiment demonstrates that the method developed here is very efficient.

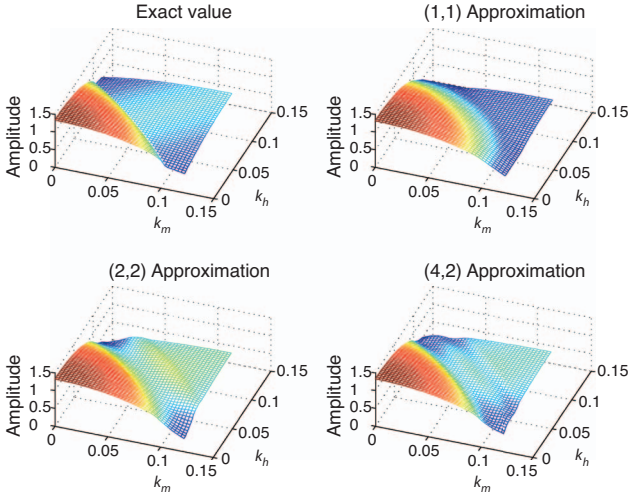

Figure 2. The exact-phase values of $\mathcal{B}_2(u(2,20),k_m,k_h)$, (1, 1), (2, 2), and (4, 2) approximations.

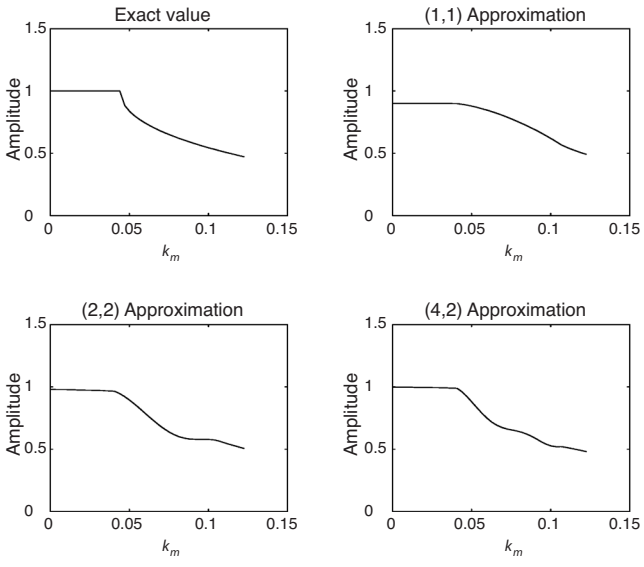

Figure 3. A 2D slice of Figure 1 for $k_h = 0.0597$.

Now we test our separable approximation on the Marmousi model. Figure 7 shows the Marmousi velocity model. Based on actual geology, the Marmousi model includes the complexities that pose challenges to migration methods. In our experiment, we use 240 shot records, each of which has 96 traces. We set $\Delta x = 12.5m, \Delta z = 4m$. In Figure 8, we show the migration result obtained by the separable approximation 20. We use the same migration procedure used by Popovici (1996). From the results, we can see that the separable approximation has the capability of imaging the regions with steeply dipping interfaces and strong lateral-velocity variations. Since the main purpose of this paper is to introduce a new method for separating the DSR operator, we will not perform comprehensive numerical implementation and comparisons. To use approximation 22, we need to develop techniques to separate the shot records. In principle, this separation of shot records can also be performed based on a singular-value decomposition technique (Ulrych et al., 1999).

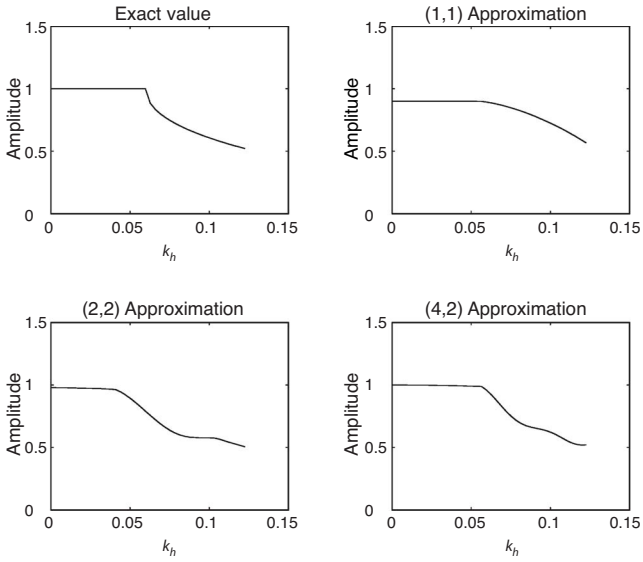

Figure 4. A 2D slice of Figure 1 for $k_m = 0.0439$.

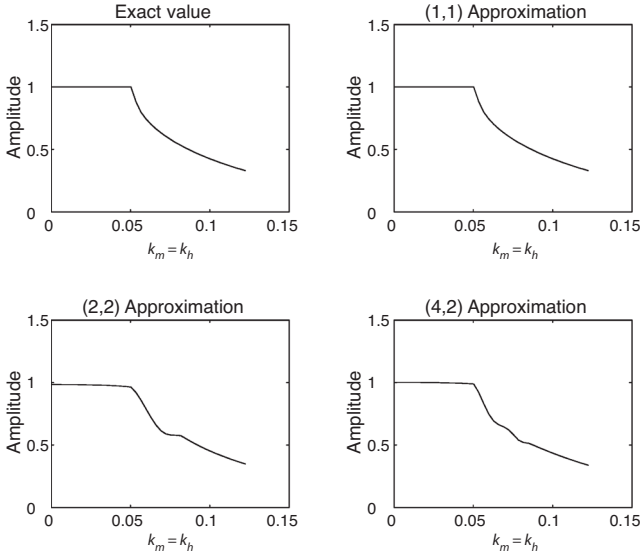

Figure 5. A 2D slice of Figure 1 for $k_m = k_h$.

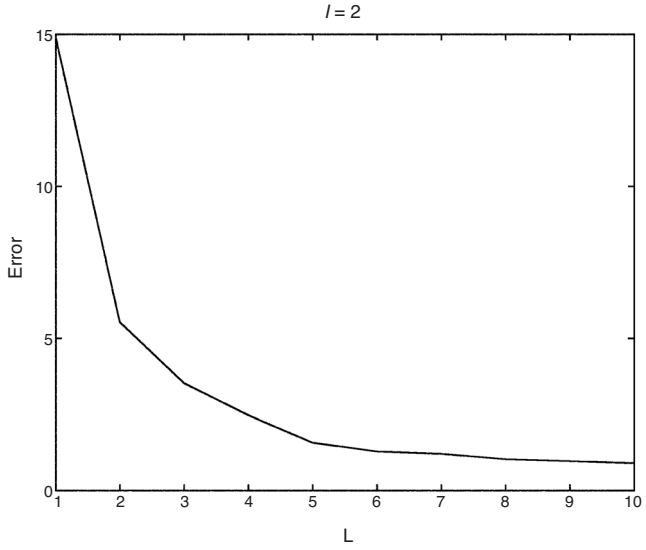

Figure 6. The errors that vary with different L for $I = 2$.

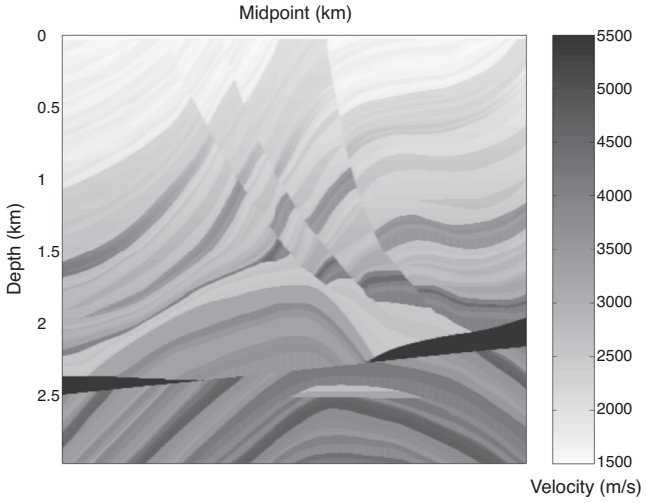

Figure 7. The Marmousi velocity model.

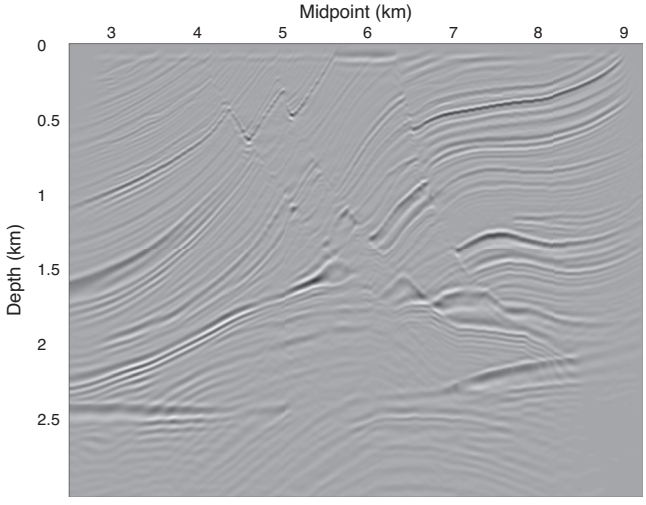

Figure 8. The migration result of the separable approximation.

CONCLUSIONS

We present a simple, but efficient separable-kernel decomposition method for approximating the DSR continuation operator. The innovative point of this method is to employ the techniques developed for linear problems to solve nonlinear problems in an indirect way. This approximation has high convergence rate, and therefore makes it possible to use high-order approximation of the continuation operator with low computational cost. Simple experiment demonstrates the feasibility of this new method to image complex geologic regions.

ACKNOWLEDGMENTS

We would like to thank the associate editor Tamas Nemeth and anonymous reviewers for valuable suggestions and corrections. This work is supported by National Natural Science Foundation of China under grant no. 40474047 and also partially by Chinese Academy of Sciences with Key Project of Knowledge Innovation KZCX1-SW-18.

APPENDIX A

EQUIVALENCE BETWEEN OPTIMIZATION AND INTEGRAL EQUATION SYSTEM

In this appendix, we prove that the optimization problem 3 can be transformed into the integral-equation problem 7. The optimization problem 3 amounts to solving the minimum problem of the functional

$$F(\phi(u),\psi(k),\lambda) = \int_a^b \int_c^d (\mathcal{A}(u,k) - \lambda\phi(u)\psi(k)^*)(\mathcal{A}(u,k)^* - \lambda^*\phi(u)^*\psi(k))dudk \tag{A-1}$$

under the constraint

$$\int_a^b \phi(u)\phi(u)^* du - 1 = 0, \quad \text{and} \quad \int_c^d \psi(k)\psi(k)^* dk - 1 = 0. \tag{A-2}$$

Construct functional

$$L(\phi(u),\psi(k),\lambda) = F(\phi(u),\psi(k),\lambda) + m_1\left(\int_a^b \phi(u)\phi(u)^* du - 1\right) + m_2\left(\int_c^d \psi(k)\psi(k)^* dk - 1\right), \tag{A-3}$$

where m_1 and m_2 are Lagrange multipliers.

The constrained-minimum problem of functional A-1 under constraint A-2 can be reduced to the unconstrained-minimum problem of functional A-3.

Let ϵ be a real parameter and $h(u)$ an arbitrary fixed function in u. From $\partial/\partial\epsilon|_{\epsilon=0} L(\phi(u) + \epsilon h(u), \psi(k), \lambda) = 0$, and equation A-2, we can obtain

$$m_1\phi(u) = \lambda^* \left[\int_c^d \mathcal{A}(u,k)\psi(k)dk - \lambda\phi(u) \right]. \quad \text{(A-4)}$$

Multiplying $\phi(u)^*$ on both sides of equation A-4, integrating over $[a,b]$, and using equation A-2 leads to

$$m_1 = \lambda^* \left[\int_a^b \int_c^d \mathcal{A}(u,k)\phi(u)^*\psi(k)dudk - \lambda \right]. \quad \text{(A-5)}$$

Let μ be an arbitrary, fixed complex number. From $\partial/\partial\epsilon|_{\epsilon=0} L(\phi(u), \psi(k), \lambda + \epsilon\mu) = 0$ and equation A-2, we can obtain

$$\lambda = \int_a^b \int_c^d \mathcal{A}(u,k)\phi(u)^*\psi(k)dudk. \quad \text{(A-6)}$$

From equations A-5 and A-6, we conclude that $m_1 = 0$. From equation A-4 and $m_1 = 0$, we finally arrive at

$$\int_c^d \mathcal{A}(u,k)\psi(k)dk = \lambda\phi(u). \quad \text{(A-7)}$$

Let $g(k)$ be an arbitrary fixed function in k. Following the same derivations, from $\partial/\partial\epsilon|_{\epsilon=0} L(\phi(u), \psi(k) + \epsilon g(k), \lambda) = 0$, we can obtain

$$\int_c^d \mathcal{A}(u,k)^*\phi(u)du = \lambda^*\psi(k). \quad \text{(A-8)}$$

Equations A-7 and A-8 constitute integral equation system 7.

In the same way, we can prove that optimization problem 18 can be transformed into integral-equation problem 19.

REFERENCES

Biondi, B., and G. Palacharla, 1996, 3-D prestack migration of common-azimuth data: Geophysics, **61**, 1822–1832.

Chen, J.-B., and H. Liu, 2004, Optimization approximation with separable variables for the one-way operator: Geophysical Research Letters, **31**, L06613.

——–, 2006, Two kinds of separable approximation for the one-way wave operator: Geophysics, **71**, no. 1, T1–T5.

Claerbout, J. F., 1985, Imaging the earth's interior: Blackwell Scientific Publications, Inc.

Jin, S., C. C. Mosher, and R.-S. Wu, 2002, Offset-domain pseudoscreen prestack depth migration: Geophysics, **67**, 1895–1902.

Le Rousseau, J. H., and M. V. de Hoop, 2001, Modelling and imaging with the scalar generalized-screen algorithms in isotropic media: Geophysics, **66**, 1551–1568.

Ortega, J., and W. Rheinboldt, 1970, Iterative solution of nonlinear equation in several variables: Academic Press Inc.

Pipkin, A. C., 1991, A course on integral equations: Springer-Verlag Inc.

Popovici, A. M., 1996, Prestack migration by split-step DSR: Geophysics, **61**, 1412–1416.

Ristow, D., and T. Rühl, 1994, Fourier finite-difference migration: Geophysics: **66**, 1882–1893.

Song, J., 2001, The optimization expression of functions and manifolds in high dimensions by ones in low dimensions: Chinese Science Bulletin, **46**, 977–984.

Stoer, J., and R. Bulirsch, 1991, Introduction to numerical analysis, 2nd ed.: Springer-Verlag Inc.

Stoffa, P. L., J. T. Fokkema, R. M. de Luna Freir, and W. P. Kessinger, 1990, Split-step Fourier migration: Geophysics, **55**, 410–421.

Ulrych, T. J., M. D. Sacchi, and J. M. Graul, 1999, Signal and noise separation: Art and science: Geophysics, **64**, 1648–1656.